

Electrosynthesis and Electrochemical Mechanism of Zn-Based Metal-Organic Frameworks

Huimin Yang, Haiyan Du, Liqin Zhang, Zhenhai Liang*, Wanjie Li

College of Chemistry and Chemical Engineering, Taiyuan University of Technology
Taiyuan, Shanxi, 030024, P.R. China

*E-mail: liangzhenh@sina.com; liangzhenhai@tyut.edu.cn

Received: 3 November 2014 / Accepted: 9 December 2014 / Published: 16 December 2014

The Zn-based MOFs which choose acrylamide and acrylic acid as organic ligand were first synthesized by an effective and versatile electrochemical method. The physical and chemical properties of the complex were characterized by atomic absorption spectrometry, FTIR, TG, XRD means, the influence of synthesis time and the effect of initiator Ce^{4+} had also been investigated. The results show that the optimal current density and reaction time for the synthetic crystals is 0.125 A/cm^2 and 1.5 h at the temperature $25\text{ }^\circ\text{C}$. Under this condition, and specific surface area of prepared Zn(acrylamide-co-acrylic acid) are 273275 , $267\text{ }^\circ\text{C}$ - $395\text{ }^\circ\text{C}$ and $186.3\text{ m}^2/\text{g}$, respectively. Meanwhile, the mechanism of the electrochemical synthesis process was investigated and the reaction course was determined through electrochemical method. The anodic and the cathodic apparent transport coefficient and derived the rate controlling step in the electrochemical synthesis process had been calculated, the role of free radicals played in the electrosynthesis reaction had also been discussed. This electrosynthesis method provides a new way for the synthesis of MOFs porous materials.

Keywords: Metal-organic frameworks, Electrosynthesis, Zn(acrylamide-co-acrylic acid), Electrochemical mechanism

1. INTRODUCTION

Metal-organic Frameworks (MOFs) materials are widespread concern as a new functional materials, it has a special advantage as compared with inorganic or organic porous materials[1]. Metal-organic frameworks porous materials have a wide application prospect in gas storage, selectivity, optical, electrical and magnetic materials and catalyst[2-7]. Currently the MOFs were mostly prepared by hydrothermal/solvothermal method which must at high temperature and pressure of high energy consumption.

Yaghi synthesized MOF-n series of metal-organic polymer by changing the ligands and central metal ions using hydrothermal method. The typical MOF-5[8] was prepared used terephthalic acid diethyl amide solution and zinc salt crystallization proceeds under 130 °C by Yaghi. MOF-177[9] was obtained by BTB (4,4-bipyridine) and $Zn(NO_3)_2 \cdot 6H_2O$ in diethyl formamide as solvent at 100 °C. Ferey, who lead France Lavoisier research group also have done a lot of research work related MOFs. For example: MIL-53[10] is the ligand complexes formed by chromium and terephthalate through hydrothermal method. Although this method solved the insoluble problem of precursor, the solvent used in the synthesis has a great selection, the reaction time is still long, and has strict requirements on reaction device.

In recent years, microwave and ultrasonic methods had been applied into the field. Lin[11] used microwave as an energy source to synthesize metal-organic polymers. But within minutes the formation of crystals, crystal growth morphology is neither good, nor the formation of single crystals.

Compared with the traditional methods which required high energy consumption and long reaction time, the electrochemical method is low consumption, easy to control and clean[12,13]. The present Mueller[14] for the first time using electrochemical method to synthesize Cu-BTC (H_3BTC : trimesic acid) metal organic polymers, Gascon[15] also prepared some archetypical Zn^{2+} , Cu^{2+} and Al^{3+} MOFs by electrochemical method at different conditions. However, these method for the preparation of metal-organic polymer was in a nitrogen atmosphere and the reaction mechanism of the electrochemical method for the preparation of MOFs materials have not been reported.

Until now, there have been no reports of the synthesis of Zn(acrylamide-co-acrylic acid) MOFs. Herein, we report the electrosynthesis process of the new Zn(acrylamide-co-acrylic acid) MOFs through the clear and simple method under atmospheric pressure and temperature conditions. Meanwhile, the mechanism of the electrosynthesis process has also been studied by electrochemistry method. This method can significantly reduce the reaction time and the demanding requirements for synthesis reaction apparatus. The prepared Zn(acrylamide-co-acrylic acid) MOFs proved that synthesizing MOFs through electrochemical method is feasible, and provided a new way for the synthesis of MOFs porous materials at mild condition.

2. EXPERIMENTAL

2.1 Preparation of Zn-based metal-organic frameworks

All chemicals were analytical grade and used without further purification. Zn plate was selected as the anode, Ti electrode as the cathode (In order to investigate the effects of different electrodes on the metal ion content in the synthetic products, we made another set of experiments, which is based on PbO_2 as anode, Ti electrode as cathode, the other reaction conditions are the same). 9.0 g acrylamide and 5 ml acrylic acid was added to a 120 ml aqueous solution containing 0.5mol/L zinc sulfate solution as the electrolyte. 0.05g ceric ammonium nitrate was add as initiator of the reaction. Then electrochemical polymerization was carried out through HB17301 SC 10A DC stabilized power after supply nitrogen for five minutes. 1.5 h later, stop energized, ethanol

was added to precipitate a polymer, filtered the polymer, and washed three times with distilled water, dried in an oven at 80 °C. The power was Zn-(acrylamide-co-acrylic acid) MOFs.

2.2 Instrumentation and analysis methods

The phases of the products were characterized by X-ray powder diffraction (XRD, Rigaku D/2500 X-ray diffraction with Cu-Kα radiatio, 10°-60°, 40 kV, and 1000 mA). SEM images were acquired using a JSM-7001F system (Jeol, Japan) operating at 10 kV. FTIR spectrum analysis was performed using a FTIR-8400S (Shimadzu, Japan) Fourier-transform infrared system. Chosen SDTA851(N₂ atmosphere, heating rate 10 °C/min, 25 °C-800 °C) as thermal gravimetric analysis instrument. Atomic absorption spectrometry (AA240Fs, VARIAN) was used to measure the content of zinc ion after the samples were digested. In accordance with GB/T 12005.3-1989, Ubbelohde viscometer of 0.5~0.6 mm was used to measure the molecular weight. Using ubbelohde viscometer detect three different times, to calculate the mean time, the calculate the molecular weight according to following formula.

The relative viscosity: $\eta_r = t/t_0, t_0=110\text{ s}$ (1)

Increase in specific viscosity: $\eta_{sp} = \eta_r - 1$ (2)

The intrinsic viscosity: $[\eta] = [2(\eta_{sp} - \ln \eta_r)]^{0.5} / C$ (3)

$[\eta] = 3.73 \times 10^{-4} M^{0.66}$ (4)

C: Test the concentration of polymer in the solution (g/100 ml) ,

C = 2 drops of test fluid volume x conversion rate.

According to Equation 2.4, the molecular weight will be calculated.

Tafel Curve and Cyclic voltammetry (CV) are used in Shanghai Chen Hua CHI660D electrochemical workstation measured the electrochemistry curves of the reaction system. All electrochemical experiments were performed in a conventional three-electrode cell system, more specifically, taking the Zn plate as anode (the working electrode), Ti cathode as the counter electrode, and SCE as the reference electrode. The electrolyte was 0.5 M ZnSO₄ (120mL) solution containing 9.0 g acrylamide, 5 ml acrylic acid and 0.05g ceric ammonium nitrate.

3. RESULTS AND DISCUSSION

3.1 Atomic absorption analysis results

Table 1. Metal ion content and absorbance of synthesis crystal under different electrode

Electrode (Anode/ Cathode)	Electrolyte	Reaction time	Concentration of metal ion (g/L)	Absorbance
----------------------------------	-------------	------------------	----------------------------------------	------------

Zn/ Ti	ZnSO ₄	2.5h	3.7274	0.2124
PbO ₂ / Ti	ZnSO ₄	2.5h	2.9232	0.1793

As can be seen from Table.1, synthetic crystals using different electrode own different metal ion content, crystal metal ion content which of zinc tablets as anode is more higher than titanium-based lead dioxide as anode. This is because that when using anode zinc tablets as anode it will dissolved at the effect of anodic oxidation, it will lead to the zinc ions in electrolyte is higher than using titanium plate as the anode [16, 17], so the reaction rate is more faster, zinc ions participating in the polymerization will also increase. Meanwhile, as the reaction proceeds, the zinc ions are consumed, the zinc ions produced by the anodic oxidation of zinc tablets will maintain the zinc ion content in the electrolyte does not decrease, keep the reaction continue, but the titanium-based lead dioxide no such effect. So metal electrode is better than oxide electrode.

3.2 SEM image

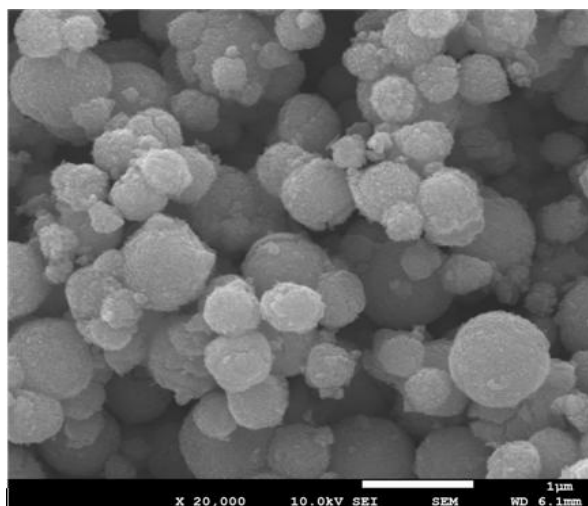


Figure 1. SEM image of the Zn (acrylamide-co-acrylic acid) MOFs

Figure. 1 shows a SEM image of a sample prepared by electro-chemical synthesis. As can be seen from the figure, Zn-based MOFs synthesized by the electrochemical method presents a distinct loose spherical structure; the diameter is about 0.5 micrometers. The electrical stimulation plays an important role in the production of the distinct loose spherical structure. In the energized condition, electrical stimulation may be due to the movement of ions leading to an oriented arrangement of Zn²⁺ and organic ligand. The electric current causing the regular arrangement of the anion and cation is different from other synthesis methods. But the size of the spheres is not very uniform, the size of spheres in the outermost layer is slightly smaller, this can be attributed to the concentration of ligand,

as the reaction proceeds, the concentration of organic ligand in the reaction system declined, the reaction rate of the coordination reaction would decreased with it.

3.3 XRD Pattern

As can be seen from the Figure.2, diffraction peaks appeared in 20.22° , 31.20° and 45.10° are attributed to the face centered cubic crystal-based (fcc)[18] Zn (101), (005), (118) crystal plane, the three peaks at 29.75° , 30.36° and 31.25° indicated that the samples is the organics containing C, H, O and N. wherein the Zn (101) crystal face diffraction peaks strongest, indicated that the Zn^{2+} has bonded in organic matter. This result is consistent with the atomic absorption analysis results.

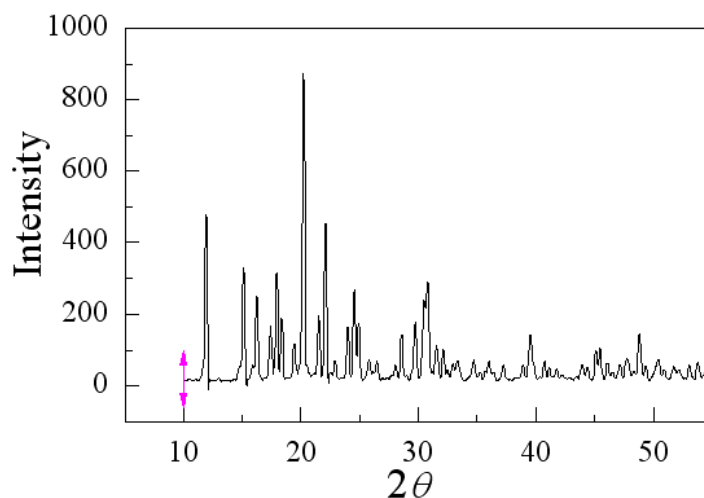


Figure 2. XRD pattern of the Zn (acrylamide-co-acrylic acid) MOFs

3.4 FTIR Analysis

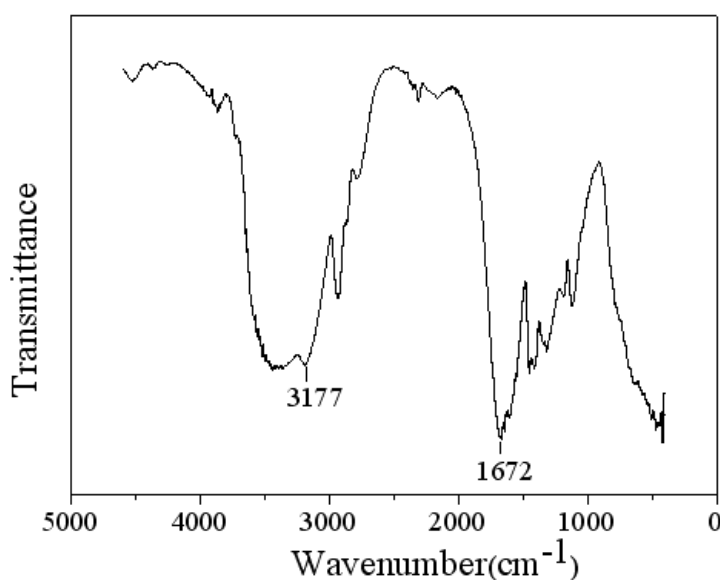


Figure 3. The FTIR of Zn(acrylamide-co-acrylic acid) MOFs

Seen from Figure 3, the absorption peak at the wavenumber 1672 cm^{-1} around can be attributed to the stretching vibration of group $\text{-C}=\text{O}$ in the amide, this is standard $\text{-C}=\text{O}$ absorption peak shift from 1690 cm^{-1} to 1672 cm^{-1} since the formation of polar bond and coordination bond between metal ions, acrylamide and acrylic acid. This result is consistent with the XRD analysis results. At the wavenumber 3177 cm^{-1} is the stretching vibration peak of -NH_2 groups [19]; From the polymer spectrum we can see that the $\text{C}=\text{C-H}$ stretching vibration peak at 990 cm^{-1} has completely disappeared, it illustrate that that polymerization of acrylamide and acrylic acid occurred in the electrosynthesis reaction.

3.5 Thermal stability analysis

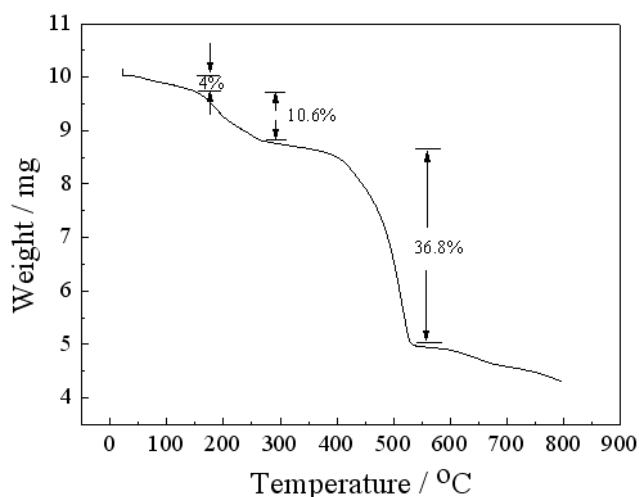


Figure 4. TG curves of the prepared Zn(acrylamide-co-acrylic acid) MOFs

It is shown from the Figure 4 that the structure of the Zn-based MOFs has better stability. There are three significant weight loss process, the first decline appeared from $30\text{ }^{\circ}\text{C}$ to the $145\text{ }^{\circ}\text{C}$, the 4% mass loss may be due to the evaporation of adsorbed water. The second loss about 10.6% is observed in $145\text{-}267\text{ }^{\circ}\text{C}$ range. The loss in mass ($\sim 10.6\%$) can be attributed to the release of crystalline waters and small molecules that are adsorbed in the holes of the prepared Zn-based MOFs. At the range of $267\text{ }^{\circ}\text{C}$ - $395\text{ }^{\circ}\text{C}$, the weight of sample keep stable, it illustrated that the stable temperature range is $267\text{ }^{\circ}\text{C}$ - $395\text{ }^{\circ}\text{C}$. The larger decline in mass (34.8%) after $395\text{ }^{\circ}\text{C}$ is mainly due to disruption in the skeleton of Zn-based MOF and its decomposition at high temperature. Above $540\text{ }^{\circ}\text{C}$, the weight of sample is not change significantly, with the final product being ZnO.

3.6 The measurement of molecular weight and the specific surface area

According to Equation 4, the molecular weight can be calculated. The calculated molecular weight of Zn(acrylamide-co-acrylic acid) is 273275. This results show that the ligand acrylamide and acrylic acid was crosslinked and ligand formed the infinite reticular structure. The specific surface area

measured by the BET measurement is $186.3 \text{ m}^2/\text{g}$. It is another evidence of the formation of a porous framework materials.

3.7 Influence of time on the yield of crystals

As can be seen from Figure 5, crystal yield increased with time increasing from 0.5 h-1.5 h, 1.5 h was the maximum, then the yield declined with the extension of time. This phenomenon maybe due to the characteristics of radical polymerization. There are two obvious feature of radical polymerization reaction[22, 23] as followed.

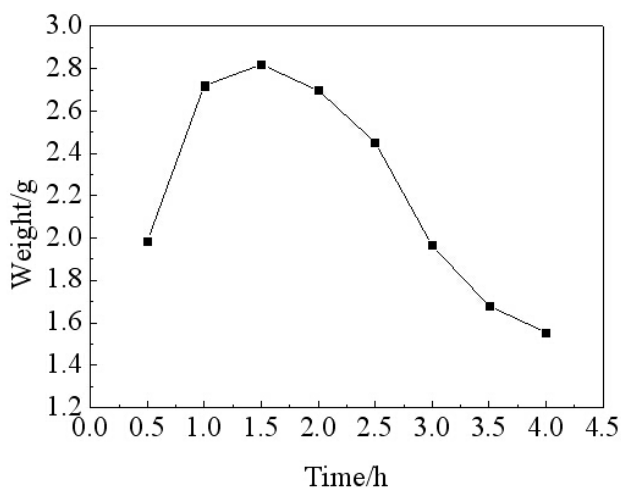


Figure 5. The relationship between Zn (acrylamide-co-acrylic acid) crystal yield and reaction time

1. Free radical polymerization process can be divided into chain initiation, chain growth, chain termination and chain transfer four basic reactions. For the reaction rate is the lowest, chain initiation is the key to control the rate of polymerization.

2. Free radical polymerization has characteristics of chain and instantaneous speed :

(1). Chain, in the radical polymerization, the monomer free radical generation, as soon as added with the second monomer, radicals generated containing two monomer units, the chain of free radical activity does not decay immediately added with the third, fourth monomer, the monomer one by one up to add rapid increase in the degree of polymerization of the chain radicals. The reaction is driven by the polymerization heat which was generated by chemical bonds type changed. Therefore, the polymerization can be a series of automatic carry on until the chain of free radical activity disappeared.

(2). Radical polymerization transient high-speed characteristics: The chain growth reaction to increase the degree of polymerization, and increase of the activation energy E_p is very low, about 20~34 (kJ/mol), so an increase of the reaction rate very high, within a few seconds to 0.01 s, there are thousands of even tens of thousands of monomers took part in the reaction, to generate a relative molecular mass for tens of thousands to hundreds of thousands of macromolecules in a very short time, is instantaneous. Polymerization system is often only the monomer and polymer the two parts, there is no the increasing degree of polymerization of a presentation of the intermediate product.

3.8 The electrochemical behavior of initiator Ce^{4+}

Figure 6 are the cyclic voltammetry curves of Zn(acrylamide-co-acrylic acid) MOFs electrosynthesis system before and after adding cerium ammonium nitrate. As can be seen from the figure, after adding Ce^{4+} , there is an obvious oxidation peak appearing, it results from the oxidation of Ce^{3+} . Contrast with the CV curve without Ce^{4+} , the reduction peaks potential moved from -1.6 V to -1.2 V, and reduction peak current intensity is also significantly improved, which can indicate that Ce^{4+} is reduced to Ce^{3+} responses easier than the system without Ce^{4+} , it also consistent with the phenomenon that experiment solution color changed from yellow to colorless.

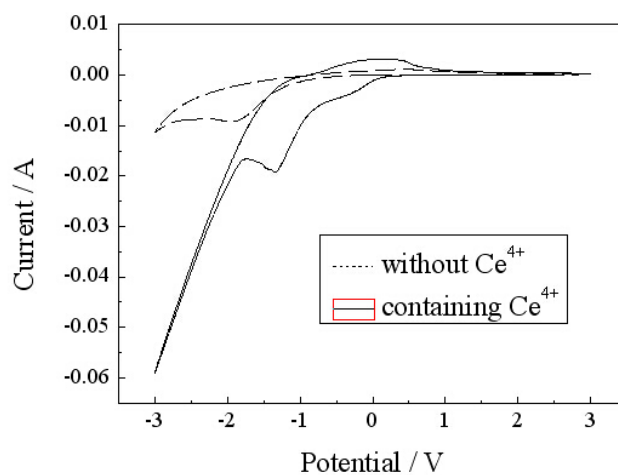


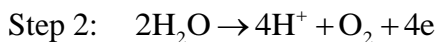
Figure 6. CV curves of the electrosynthesis Zn-(acrylamide-co-acrylic acid) MOFs system before and after adding cerium ammonium nitrate ($\nu=50 \text{ mV}\cdot\text{S}^{-1}$)

The results described the initial initiator Ce^{4+} is required in the electro-polymerization Zn (acrylamide-co-acrylic acid) system, and under the synergistic effect of electrochemical reaction and initiator Ce^{4+} , the synthesis system produces large amounts of free radicals[24], triggering acrylamide and acrylic acid polymerization to form P (acrylamide-co-acrylic acid), and then bonding with Zn^{2+} . Meanwhile initiator Ce^{4+} is reduced to Ce^{3+} , the followed was the electrochemical oxidation of Ce^{3+} and form Ce^{4+} ions, Ce^{4+} continue to play initiator role, so the loop[25], the continuous generation of free radicals, and continuously polymerized to form a Zn infinite network structure (acrylamide-co-acrylic acid).

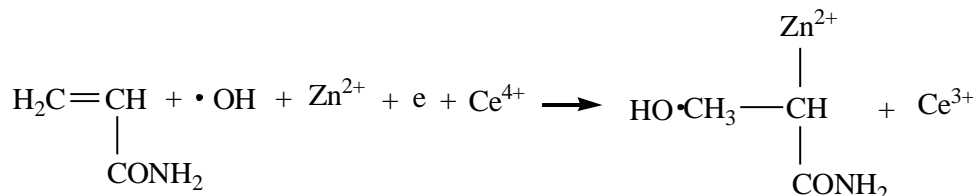
3.9 Determination of the electrode reaction process and the intended reaction

The electrochemical reaction is one of the most powerful redox reaction. There is no doubt that zinc anode occur anodic oxidation reaction to produce Zn^{2+} ion, this can be confirmed from the experimental phenomenon of anodic gradually dissolved. Meanwhile, the cathode and anode have bubbles, it may account for the electrolysis of water. There are bright metal plating appeared on the surface of the cathode, it can be attributed to the reduction reaction of Zn^{2+} ions. The polymerization of

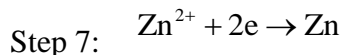
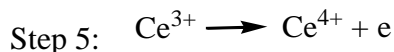
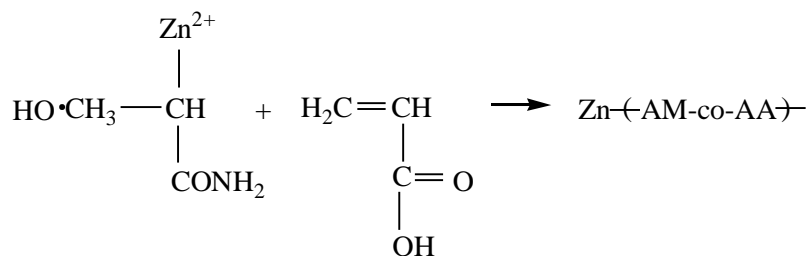
acrylamide and acrylic acid is coordination reaction, J. Yu[26] proposed a mechanism for the synthesis of P(acrylamide-co-acrylic acid) hydrogel. According to the experimental results and general rule of oxidation and coordination reaction, the reaction mechanism of the electrode may be suggested as the following:



Step 3:



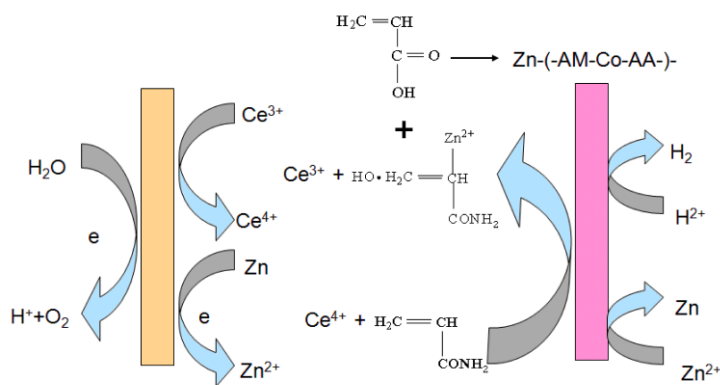
Step 4:



The total reaction can be presented as



The electrode process can be represented in the scheme 1.



Scheme 1 Schematic of the electrosynthesis reaction mechanism.

3.9.1 Reaction parameters of the measuring electrode

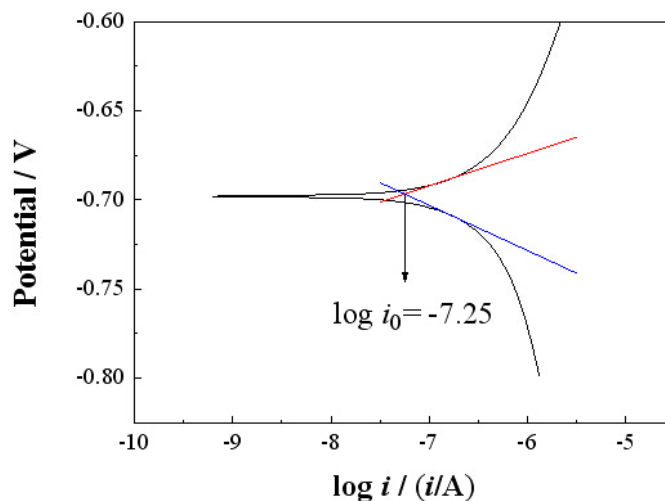


Figure 7. Stable polarization curves of the reaction (reaction solution as electrolyte, scan rate is 1mV/s)

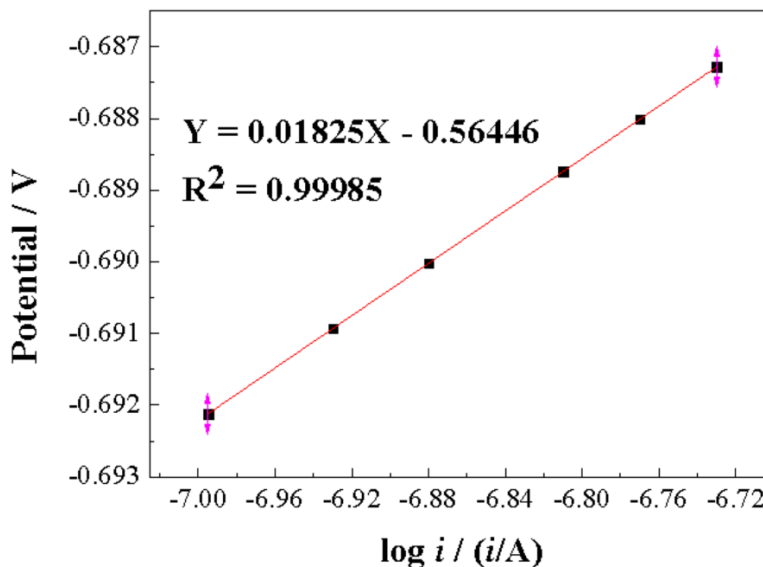


Figure 8. The anodic steady polarization curves (the condition was the same with Figure 7)

Figure 7 was the stable polarization curve of the reaction, from the figure we can get the exchange current density $\log i_0 = -7.25$.

Figure 8 was anodic steady polarization curves, anodic Tafel slope can be obtained from the curve:

$$\frac{d(\Delta\varphi)}{d\log i} = \frac{2.303RT}{\alpha F} = 0.01825(V) \tag{6}$$

So, the anode apparent transfer coefficient $\alpha = 3.24$

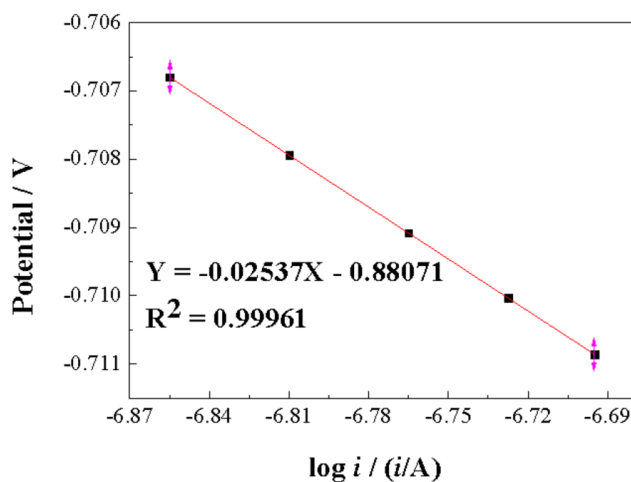


Figure 9. The cathode steady polarization curves (the condition was the same with Figure 7)

Figure 9 was cathode steady polarization curves, cathode Tafel slope can be obtained from the curve:

Similarly, the obtained cathode Tafel slope is :

$$\frac{d(-\Delta\phi)}{d\log i} = \frac{2.303RT}{\alpha F} = 0.02537(\text{V}) \quad (7)$$

So, the cathode apparent transfer coefficient $\alpha = 2.33$

Measured from the above α , α values, and generate 1 mol polymers consumes 6 mol electrons, the stoichiometry number of control steps is :

$$v = \frac{6}{\alpha + \alpha} = \frac{6}{3.24 + 2.33} \approx 1 \quad (8)$$

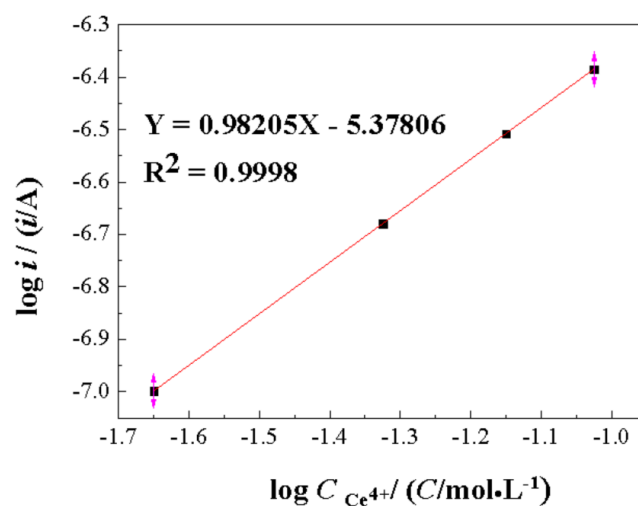


Figure 10. Relationship between Ce⁴⁺ ion concentration and current

Figure 10 was the relationship between Ce⁴⁺ ion concentration and current which got from the tafel curves at different Ce⁴⁺ ion concentration. From the figure, we can calculated the anodic electrochemical reaction order of Ce⁴⁺ approximately equal to 1 .

$$Z_{Ce^{4+},c} = \left(\frac{d \log i}{d \log c_{Ce^{4+}}} \right)_{\phi,p,H,T} = 0.98205 \approx 1 \quad (9)$$

3.9.2 The derivation of reaction mechanism

Similarly with chemical reactions, the dynamics relationship of organic electrosynthesis reaction electrode can also be deduced by steady state law or quasi-steady-state equilibrium method. The basic assumption of the steady-state law[27] is that under steady-state conditions, the concentration of the chemical reactants are constant. The basic assumption of the quasi-equilibrium method[28] is that under steady-state conditions, the reaction step are in equilibrium except the control step. When only one determined step in the plurality of reaction steps, quasi-equilibrium method can be used. In the electrochemical polymerization process of Zn(acrylamide-co-acrylic acid), only one step controlling the rate of reaction, so the following derivation using the quasi-equilibrium method.

Assume that the step 3 is the rate controlling step :

Relationship between current and potential can be drawn:

$$i = \bar{i} - \bar{i} = 6F \left\{ 2K_1 \exp \left[\frac{(-2-\alpha)F\phi}{RT} \right] C_{Ce^{4+}} - K_2 C_{Ce^{4+}} \exp \left[\frac{(3-\alpha)F\phi}{RT} \right] \right\} \quad (10)$$

Assuming the anodic polarization is large enough, that is $\eta \geq 120/n$ (mV), the cathode reaction can be ignored, the current density for anode reaction can be :

$$i = \bar{i} - \bar{i} = 12FK_1 \left[\frac{(-2-\alpha)F\phi}{RT} \right] C_{Ce^{4+}} \quad (11)$$

It can be seen from equation (11), anodic electrochemical reaction order of Ce⁴⁺ is 1. It is consistent with the experimental reaction order. So the step 3 is the control step.

According to the mechanism based on assumptions, the apparent transfer coefficients of anode and cathode can be calculated. First, we can get the value of $\vec{\gamma}$, ν , n and r from the assuming directly, meanwhile assuming $\alpha=0.5$, the calculated process as follows:

When the step 3 is the rate controlling step :

$$\vec{r} = 3, r = 1, \nu = 1, n = 6$$

$$\vec{\alpha}_1 = \frac{\vec{\gamma}}{\nu} + ar = 3.5$$

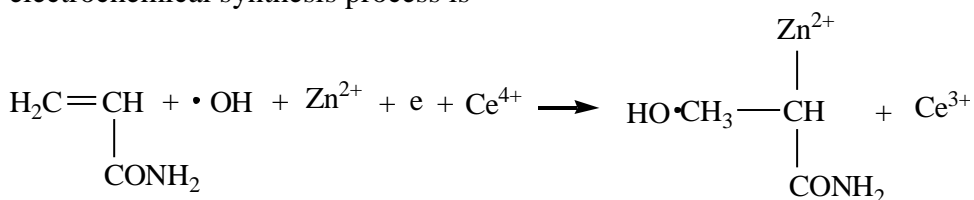
$$\overleftarrow{\alpha}_1 = \frac{n - \vec{\gamma}}{\nu} - ar = 2.5$$

Compared the calculated value of the apparent transfer coefficient is in agreement with the experimental values, its further it's further prove electrode reaction mechanism identified above is correct.

As can be seen from the mechanism derivation, in the process of electrochemical synthesis Zn(acrylamide-co-acrylic acid), the formation of monomer radical reaction through electron transfer process caused by hydroxyl radical monomer is the control step, it's the further evidence of the important role of hydroxyl radicals. We can guide the synthesis experiment by adjusting the reaction rate of the controlling step, improve the conversion rate of reaction.

4. CONCLUSIONS

The Zn(acrylamide-co-acrylic acid) MOFs were successfully synthesized using electrochemical method and the mechanism of the electrosynthesis reaction was also investigated. The physical and chemical properties of these complexes were characterized by Atomic absorption spectrometry, FTIR, TG, XRD means, the influence of synthesis time and the effect of initiator Ce^{4+} had also been investigated. The results show that: the initial initiator Ce^{4+} is required in the electro-polymerization Zn(acrylamide-co-acrylic acid) system, the optimal current density and reaction time for the synthetic crystals is 0.125 A/cm^2 and 1.5 h at the temperature $25\text{ }^\circ\text{C}$. The XRD and FTIR results that metal ion bonded to the polymer. Under this condition, the molecular weight, stable temperature and specific surface area of Zn(acrylamide-co-acrylic acid) are 273275, $267\text{ }^\circ\text{C}$ - $395\text{ }^\circ\text{C}$ and $186.3\text{ m}^2/\text{g}$, respectively. The reaction course was determined through electrochemical method. The calculated anodic and the cathodic apparent transport coefficient were 3.24, 2.33 respectively. The rate controlling step in the electrochemical synthesis process is



Free radicals play important role in the electrosynthesis reaction. This electrosynthesis method provides a new way for the synthesis of MOFs porous materials.

ACKNOWLEDGEMENT

This work is jointly funded by the National Natural Science Foundation of China and Shenhua Group Corp. (Grant nos. U1261103) and the Technological Project of Shanxi Province (20100311033). The authors thank for anonymous reviewers for their helpful suggestions on the quality improvement of our present paper.

References

1. S.C. Sahoo, T. Kundu and R. Banerjee, *J. Am. Chem. Soc.*, 133(2011)17950.
2. A. G. Wong-Foy, A. J. Matzger and O. M. Yaghi, *J. Am. Chem. Soc.*, 128(2006)3494.
3. Z. J. Zhang, W. Y. Gao, L. Wojtas, S. Q. Ma, M. Eddaoudi and M.J. Zaworotko, *Angew. Chem. Int. Ed.*, 51(2012)9330.
4. S. Pramanik, Z.C. Hu, X. Zhang, C. Zheng, S. Kelly and J. Li, *Chem. Eur. J.*, 2013, 19(2013)15964.

5. L. Shen, S.W. Yang, S.C. Xiang, T. Liu, B.C. Zhao and M.F. Ngetal, *J. Am. Chem. Soc.*, 134(2012)17286.
6. F. Stallmach, S. Groger, V. Kunzel, J. Karger, O.M. Yaghi, M. Hesse and U. Muller, *Angew. Chem. Int. Ed.*, 45(2006)2123.
7. M. Sabo, A. Henschel, H. Froede, E. Klemm and S. Kaskel, *J. Mater. Chem.*, 17(2007) 3827.
8. A.H. Yuan, X.P. Shen, K.B. Yu, L.D. Lu, W. Zhou and J. Zhong, *Acta. Chim. Sini.*, 61(2003)1603.
9. H. Li, M. Eddaoudi, M.O. Keeffe and O.M. Yaghi, *Nature*, 402(1999)276.
10. F. Millange, C. Serre and G. Ferey, *Chem. Commun.*, 8(2002)822.
11. Z. Lin, D.S. Wragg and R.E. Morris, *Chem. Commun.* 19(2006)2021.
12. R.C. Tom, D. Gert, A. Rob and E. Dirk, *Micropor. Mesopor. Mat.*, 158(2012)209.
13. R. Senthil Kumar, S. Senthil Kumar and M. Anbu Kulandainathan, *Micropor. Mesopor. Mat.*, 168(2013)57.
14. U. Mueller, M. Schubert, F. Teich, H. Puetter, K. Schierle-Arndt and J. Pastre, *J. Mater. Chem.*, 16(2006)626.
15. A.M. Joaristi, J. Juan-Alcaniz, P. Serra-Crespo, F. Kapteijn and J. Gascon, *Cryst. Growth. Des.*, 12(2012)3489.
16. H. Masaru and K. Hiroyuki. 2012, WO 2012001979
17. D.M. Michela, M. Matilda, M. Piero, R. Antonino, P Chiara and L Cristina. *J. Mole. Cat. A.*, 366(2013)186.
18. S. Najafi Nobar and S. Farooq, *Angew. Chem. Int. Ed.*, 2012, 51(2012)5638.
19. Y.H. Shen, X.Y. Zhang, J.J. Lu, A.Q. Zhang, K. Chen and X.Q. Li. *Colloid Surface A.*, 350(2009)87.
20. S. Najafi Nobar and S. Farooq. *Chem. Engin. Sci.*, 84(2012)801.
21. D.J. Tranchemontagne, J.R. Hunt and O.M. Yaghi. *Tetrahedron.*, 64(2008)8553.
22. S.K. Mehdi, H.A. Vahid, R.R. Saeid, B.S. Farid and R.M. Hossein. *Int J Polym Mater Polym Biomater.*, 62(2013)336.
23. V. Strehmel, A. Laschewsky and H. Wetzel. *Macromolecules*, 39(2006)923.
24. R. Liang and M.Z. Liu. *J. Agric. Food. Chem.*, 54(2006)1392.
25. I. Kaur, R. Kumar and N. Sharma. *Carbohydr. Res.*, 345(2010) 2164.
26. J. Yu, G.G. Yang, Y.P. Pan, Q.F. Lu, W. Yang, J.Z. Gao, *Plasma. Sci. Technol.* 16(2014)767.
27. W.R. Haoa, J.D. Hauenstein, C.W. Shu, A.J. Sommese, Z.L. Xu, Y.T. Zhang, *J. Computa. Phys.*, 250(2013)332.
28. F.Q. Xia and X.P. Ding. *Appl. Math. Compu.*, 188(2007)173.